FP-Experiment: Nuclear Magnetic Resonance in the Earth's Magnetic Field (EFNMR) Protocol

Robin Marzucca, Andreas Liehl

30/01/13

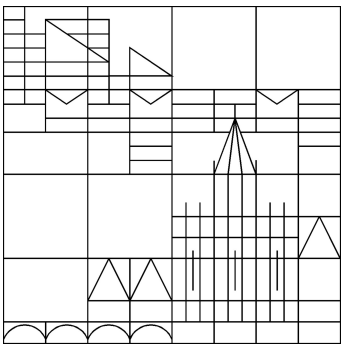

University of Constance

Abstract

Studying the atomic structure of matter, one finds that particles like electrons or nucleons has an own angular momentum, called spin. Due to the charge of these particles, the spin interacts with external magnetic fields in such a way that spin and magnetic field point into the same direction. In case of EFNMR, the external field is given by Earth's magnetic field. In nuclear magnetic resonance (NMR) one uses the interaction in such a way that one applies another oscillating magnetic field perpendicular to the external field, and therefore the spin is forced to this direction. Turning off this oscillating field, the spin aligns into its primary direction. Due to the dependence of this alignment to the matter, one can find out which material is reviewed. In our experiment we'll study the EFNMR of water, oil and $CuSo_4$.

Development of the several parts:
Abstract: A.L.
Basics: A.L., R.M.
Analysis: R.M., A.L.
Discussion of the results: R.M., A.L.

Contents

1 Introduction

Nuclear magnetic resonance (NMR in the following) describes the interaction between the magnetic moment of nucleons with an external magnetic field which oscillates with a radio frequency (RF). The interaction causes a precession movement of the atomic magnetic moment around a fixed axis, defined as z-axis.
When turning off the external magnetic field, the atomic magnetic moment is no longer dependent on external influences and can shade slowly into its primarily position. Due to the dependence of this process on the reviewed material at hand, it's possible to do some conclusions about the material.
In this way, NMR became an important method in lots of areas, e.g. in chemistry to analyse some unknown substances with the so-called nuclear magnetic resonance spectroscopy or in medicine with the so-called nuclear spin tomography, an imaging method in modern medicine. Especially the application of NMR in medicine is a big technical progress. Since NMR only works with magnetic fields, there's no destruction of cells in the body in contrast to conventional imaging methods which work with x-rays.

2 Basics

2.1 Nuclear Spin And Larmor Precession

Analogically to the electron spin $\vec{S}$ which was found out by the Stern-Gerlach-Experiment, one finds that nucleons have a spin, too, while the spin of a nucleus is denoted by $\vec{I}$. A spin can be interpreted as intrinsic angular momentum. In quantum mechanics, one finds that spin is quantized in such a way that the absolute value of the nuclear spin $|\vec{I}|$ can be written as:

$$|\vec{I}| = \hbar\sqrt{I(I+1)}$$

where I represents the quantum number of the nuclear spin which can be half-integral or integral. Analogically to the case of electrons, one defines a special axis[1], usually the z-axis, and finds out that in this direction the component of nuclear spin is quantized as well. Thus, it's:

$$I_z = \hbar m_I$$

where m_I is the magnetic quantum number with values of $m_I \in \{-I, -(I+1), \ldots, I-1, I\}$.

Furthermore, one finds that there's an interaction of nucleons respectively nuclei with an external magnetic field. This fact is explained by the standard model. The standard model is a fundamental theory of the composition of matter. One part of it is the so-called quark theory which says that nucleons are not the fundamental parts of matter but rather have a substructure. Neutrons and protons are built by so-called up- and down-quarks with charges of $q_u = \frac{2}{3}e$ and $q_d = -\frac{1}{3}e$. Therefore, a proton has a composition of two up-quarks and one down-quark which causes a charge of $q_p = e$ and analogically a neutron is built by two down-quarks and one up-quark which causes a charge of $q_n = 0$. Nevertheless,

[1] Afterwards, when regarding magnetic fields, we'll define the axis of the magnetic field as z-axis.

both nucleons are built by charged particles and therefore, analogically to charged classical particles, they have a magnetic moment. With a quantum mechanical consideration one finds for the magnetic moment of nuclei:

$$\vec{\mu}_I = g_I \cdot \frac{\mu_B}{\hbar} \cdot \vec{I} = \gamma_I \cdot \vec{I}$$

where g_I is the LANDÉ factor of the nuclei and γ_I the gyromagnetic ratio of it.
Thus, there's an additional potential energy when a nucleus is inside of an external magnetic field $\vec{B}_{\text{ext}}$. Assuming a homogeneous field and defining the direction of this field as z-axis, we can write:

$$E_{\text{mag}} = -\vec{\mu}_I \cdot \vec{B}_{\text{ext}} = -\mu_{I,z} \cdot B_z = -\gamma_I \hbar m_I B_{z,\text{ext}} \tag{1}$$

Therefore, the energy levels are split and for neighboured levels with $\Delta m_I = 1$ it's:

$$\Delta E = \gamma_I \hbar B_{z,\text{ext}} \tag{2}$$

This phenomena is called the nuclear ZEEMAN effect and one sees that without an external field, the energy levels are quite degenerated.

Another important consequence of the interaction between the external magnetic field and the atomic magnetic momentum is the so-called LARMOR precession. If $\vec{\mu}_I$ and $\vec{B}_{\text{ext}}$ are not parallel, the atomic magnetic momentum feels a torque and therefore, the magnetic moment does a precession movement around the z-axis. Thus, we can write:

$$\frac{\mathrm{d}\vec{\mu}_I}{\mathrm{d}t} = \gamma_I \vec{\mu}_I \times \vec{B}_{\text{ext}} \tag{3}$$

Note that since $\vec{B}_{\text{ext}} = (0, 0, B_{z,\text{ext}})^T$, the z-component of $\vec{\mu}_I$ is constant. As a consequence of equation (3), $\vec{\mu}_I$ precesses around the z-axis with the LARMOR frequency:

$$\omega_L = \gamma_I B_{z,\text{ext}} \tag{4}$$

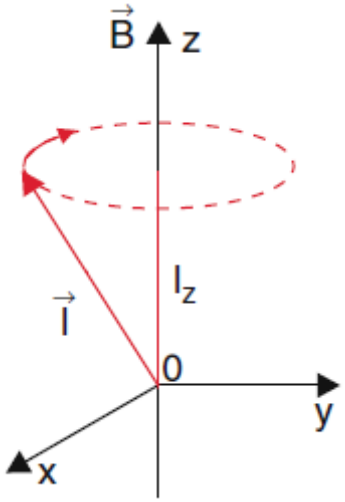

Figure 1: The sketch visualizes the LARMOR precession of an atomic magnetic moment. [Dem10]

This is also shown in figure (1).
Comparing equations (2) and (4) one sees that since the quantization of the electromagnetic field by PLANCK $E = \hbar\omega$, the LARMOR frequency is the resonance frequency[2].

2.2 Nuclear magnetic resonance (NMR)

The concept of NMR bases on the precession movement with the LARMOR frequency of the atomic spins like we have discussed in the last chapter. One tries to influence this movement while applying an external oscillating magnetic field with $\omega \approx \omega_L$. But first, we should have a look at the macroscopic magnetisation of matter.
Like we have seen in the last chapter, the z-component of nucleon spins can take different values. One finds that the distribution of these spins is not quite random. In general, the spins are predominantly in an energetically favourable state which is the state of the lowest energy. De facto, the distributed states of spin are described by the MAXWELL BOLTZMANN distribution. Therefore, the probability that a nucleon is in state j is proportional to the BOLTZMANN factor $e^{-\frac{E_j}{k_B T}}$ where E_j is the energy of state j, calculated by formula (1), k_B the BOLTZMANN's constant and T the temperature. Considering that the probability is normed, it's the probability that a nucleon is in state j:

$$p_j = \frac{\exp\left(-\frac{E_j}{k_B T}\right)}{\sum_j \exp\left(-\frac{E_j}{k_B T}\right)} = \frac{\exp\left(\frac{\gamma_I \hbar m_{I,j} B_z}{k_B T}\right)}{\sum_j \exp\left(\frac{\gamma_I \hbar m_{I,j} B_z}{k_B T}\right)}$$

Therefore, the expected value for the atomic magnetic moment $\langle \vec{\mu}_I \rangle$ is not quite zero and there's a macroscopic magnetisation $\vec{M} = N \langle \vec{\mu}_I \rangle$, where N is the number of nucleons in the material. One can consider that the magnetisation is parallel to z-axis which means parallel to the external magnetic field $\vec{B}_{\text{ext}}$. This fact is illustrated by figure (2). One sees that due to the precession movement of the spins, the components perpendicular to z-direction cancels each other.

[2] In reality, due to the fact that the LARMOR precession cause another atomic magnetic field, the external field $\vec{B}$ is overlain by it but since the discrepancy is smaller than one percent, this consideration is skipped here.

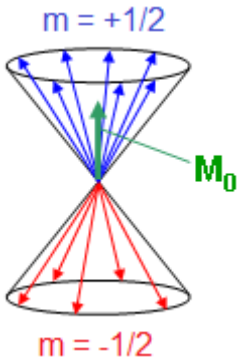

Figure 2: The sketch shows the fact that the macroscopic magnetisation is parallel to z-axis. For simplicity, we have assumed a two spin system with spin up and spin down. [UD13]

To do the mathematical description much easier, one switches from the laboratory system Σ in a coordinate system Σ' which rotates with the LARMOR frequency $\vec{\omega}_L$ around the z-axis. Then, equation (3) can be written as:

$$\begin{aligned}\left(\frac{\mathrm{d}\vec{\mu}}{\mathrm{d}t}\right)' &= \frac{\mathrm{d}\vec{\mu}}{\mathrm{d}t} - \vec{\omega}_L \times \vec{\mu} \\ &\overset{(3),(4)}{=} (\vec{\omega}_L - \vec{\omega}_L) \times \vec{\mu} \\ &= 0 \end{aligned} \tag{5}$$

so the dependence of $\vec{\mu}$ of the external magnetic field $\vec{B}_{\text{ext}}$ is eliminated and therefore $\vec{M}$ is static in this reference system Σ'.
Now, if we apply a with LARMOR frequency oscillating magnetic field, written as $\vec{B}_1(t) = (B_1 \cos(\omega_{RF} t), B_1 \sin(\omega_{RF} t), 0)^T$[3], the magnetisation $\vec{M}$ feels a static field in the rotating coordinate system which points into a specified axis which can be defined as x-axis. We obtain [TUD09]:

$$\vec{B}' = \begin{pmatrix} B_1 \\ 0 \\ B_{z,\text{ext}} + \frac{\omega_{RF}}{\gamma} \end{pmatrix}$$

Usually, one chooses $\omega_{RF} = \omega_L$, the case of resonance and therefore, the frequency in Σ' is transformed by:

$$\vec{\omega}' = \gamma \vec{B}' = \omega_1 \vec{e}_x'$$

while $\omega_1 = \gamma B_1$. We obtain the macroscopic equation of motion for the magnetisation $\vec{M}$ in Σ':

$$\left(\frac{\mathrm{d}\vec{M}}{\mathrm{d}t}\right)' = \vec{M} \times \vec{\omega}' \tag{6}$$

In case of resonance and with the starting condition $\vec{M}'(t=0) = M_0 \vec{e}_z$, equation (6) is solved by:

$$\vec{M}'(t) = \begin{pmatrix} 0 \\ M_0 \cos(\omega_1 t) \\ M_0 \sin(\omega_1 t) \end{pmatrix}$$

Thus, in Σ' the magnetisation gets an oscillating y-component and precesses around the x-axis. Otherwise, in the laboratory system Σ, the magnetisation moves on a coil on a sphere, called BLOCH sphere. These two motions are shown in figure (3). At this point, we remark that since one tries to control the additional y-component of the magnetisation one gets in the laboratory system, the frequency of the oscillating field should be much smaller than the LARMOR frequency. For this reason one chooses $B_1 \ll B_{\text{ext}}$. Otherwise, the oscillating of the y-component would be faster than the precession around the z-axis and therefore, one doesn't get the coil motion as it's shown in figure (3) as well.

[3] Note, that due to in ordinary NMR the frequencies being in ranges of radio frequency, the frequency of the oscillating magnetic field is denoted by ω_{RF}.

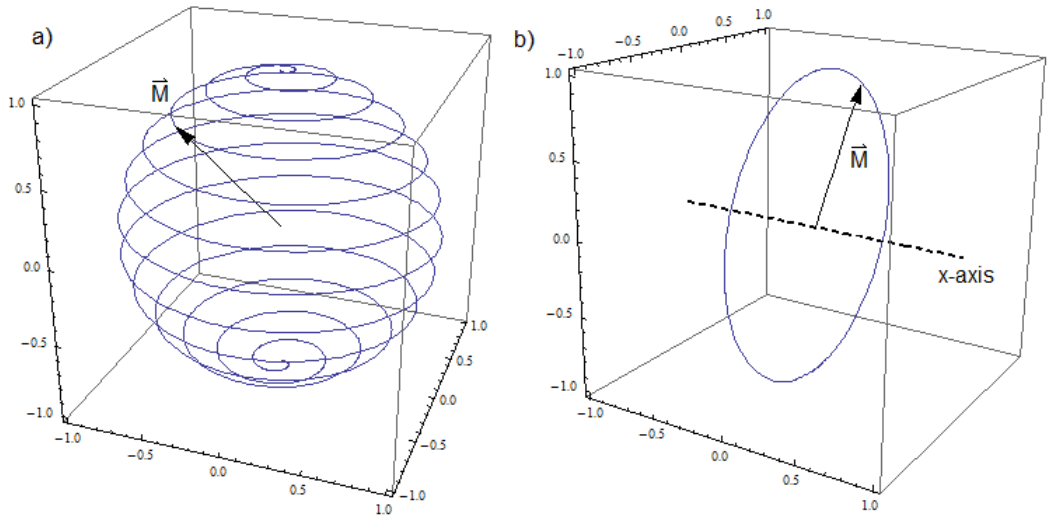

Figure 3: The sketch shows the motion of magnetisation in a) Σ and b) Σ'.

If one applies an oscillating magnetic field only for a short time, one speaks about a pulse. A pulse causes a rotation of the magnetisation and afterwards the magnetisation precesses around the z-axis. The rotation angle β of a pulse with length τ can be computed by:

$$\alpha = \tau\gamma B_1$$

In our experiment we'll use two special kinds of pulses. Firstly, a 90°-pulse which rotates the magnetisation by 90° and afterwards $\vec{M}$ precesses around the z-axis in the xy-plane. Secondly, a 180°-Pulse which only flips the magnetisation. After turning off the pulse, the magnetisation drops back into equilibrium. For a completely mathematical description of these processes, one needs lots of calculations and therefore it's skipped at this point. For simplicity, one assumes an exponential decay and in our experiment we'll see that the physics is nearly well reproduced with this approach. Therefore, the equation of motion can be written as:

$$\frac{\mathrm{d}\vec{M}}{\mathrm{d}t} = \gamma\vec{M} \times \vec{B} - \begin{pmatrix} \frac{M_x}{T_2^*} \\ \frac{M_y}{T_2^*} \\ \frac{M_z - M_0}{T_1} \end{pmatrix} \tag{7}$$

where $\vec{B}$ represents the whole magnetic field. At this point, we have established T_1 and T_2^* as heuristic relaxation times. Equation (7) is also known as Bloch equation. In the next chapter we'll explain the two relaxation times.

Prior to this we'll explain shortly the advantage of EFNMR against to NMR. In our experiment we use the Earth's magnetic field as external static field. The Earth's magnetic field has a strength about $B_E \approx 40\,\mu\mathrm{T}$. Usually, in NMR the static fields are much stronger. Therefore, the necessary resonance frequency $\omega_L = \gamma B_E$ is much lower and easier to generate.

2.3 Relaxation Processes

In general, relaxation means the process when a consciously disequilibrated system drops back to equilibrium. In case of NMR/EFNMR one speaks about the relaxation time of the spins dropping back into it's primarily position parallel to z-axis. One differs two cases: the longitudinal relaxation and the transversal relaxation.

2.3.1 Longitudinal Relaxation

Like we have discussed in the last chapter, with applying a fast oscillating magnetic field, the static magnetisation parallel to z-axis begins to precess around the x-axis. The longitudinal relaxation, also called spin-lattice relaxation, describes the movement in z-direction. Thus, we have a look at the z-component of Bloch equation (7). Since the Earth's magnetic field is very small, it's negligible and we obtain:

$$\begin{aligned} \frac{\mathrm{d}M_z}{\mathrm{d}t} &= -\frac{M_z - M_0}{T_1} \\ M_z(t) &= M_0 + (M_z(0) - M_0)\, e^{-\frac{t}{T_1}} \end{aligned} \tag{8}$$

Note that $M_z(0) \neq M_0$ cause time $t = 0$ is defined as the moment when the pulse is cut off. Using a 90°-pulse, $M_z(0)$ vanishes and it's:

$$M_{z,90}(t) = M_0 \left(1 - e^{-\frac{t}{T_1}}\right) \tag{9}$$

Otherwise, using a 180°-pulse, $M_z(0) = -M_0$ and it's:

$$M_{z,180}(t) = M_0 \left(1 - 2e^{-\frac{t}{T_1}}\right) \tag{10}$$

In the experiment the initial magnetisation M_0 is caused by Earth's magnetic field. Since it's rather weak, one amplifies it by a polarisation coil. This coil causes an additional magnetisation M_p which is polarized in y-direction. After turning off the pulse of the polarisation coil, the magnetisation which is increased now aligns oneself with z-direction again. Since $M_0 \ll M_p$, in case of a 90°-pulse, equation (9) can be written as:

$$M_{z,90}(t) = M_p \left(1 - e^{-\frac{t}{T_1}}\right) \tag{11}$$

The process of gain of the initial magnetisation is also shown in figure (4).

In physics, the spin-lattice relaxation describes the energy transfer between the magnetisation and the lattice: Since the magnetisation is not in at equilibrium, its energy is a bit higher. Therefore, when dropping back into equilibrium, the magnetisation releases energy to the surrounding lattice.

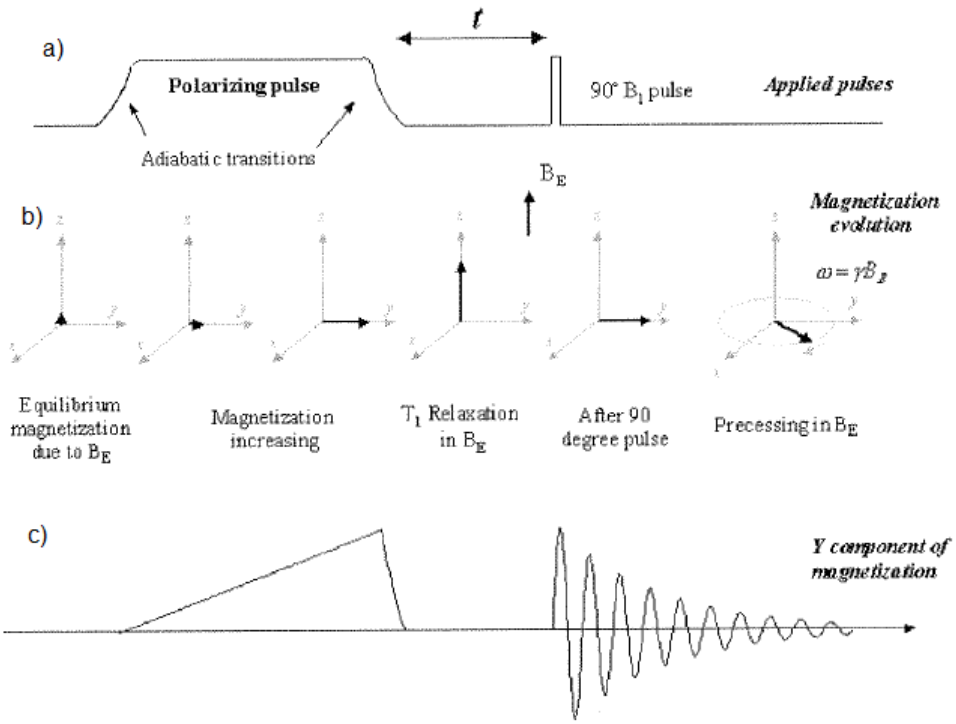

Figure 4: The figure shows the process of gain of the initial magnetic field and moreover the application of a 90°-pulse. It's a) the sequence of the necessary pulses, b) the resulting magnetisation and c) the y-component of it. [Hal06]

2.3.2 Transversal Relaxation

In contrast to longitudinal relaxation, transversal relaxation describes the relaxation of the x- and y-component. Analogically to equation (8) one solves the BLOCH equation (7) but in this case for x- and y-component. As above one neglects the influence of the Earth's magnetic field which is rather small and finds out:

$$S(t) = S_0 e^{-\frac{t}{T_2^*}} \tag{12}$$

where S describes either the x- or the y-component.
In physics, the transversal relaxation describes the fact that the several atomic magnetic moments are not in phase. According to the spin-spin-interaction, the spins of a nucleus become de-coherent and as a consequence, time after time the magnetisation vanishes. One can imagine a material which was influenced by a 90°-pulse while there's no spin-lattice relaxation[4]. Now, the spins precess in the xy-plane around the z-axis and due to the interaction between neighboured spins, some of them precess faster and others more slowly. Usually, this process runs faster than the spin lattice relaxation. We remark that we have noted the characteristic time of this process with T_2^*, because the spin-spin-interaction is not the only reason for the disappearance of the transversal component. Additionally, there are some other processes, predominantly the inhomogeneity of the magnetic field.

[4]Of course, such a system doesn't exist, because spin-lattice relaxation vanishes never but to understand the spin-spin relaxation one can assume this.

Thus, it's:

$$\frac{1}{T_2^*} = \frac{1}{T_2} + \frac{1}{T_{\text{env}}} \overset{(*)}{=} \frac{1}{T_2} + \gamma \Delta B \tag{13}$$

while T_2 is the time constant from the spin-spin-interaction and T_{env} considers all other effects in the environment. In step $(*)$ we have assumed that the main part of the other effects is the part of the inhomogeneous magnetic field, described by ΔB, and all other influences are negligible.

Since one is interested in the relaxation time T_2 caused by the spin-spin-interaction, it's not quite sufficient to measure T_2^* analogically to T_1, because the inhomogeneity of the magnetic field is not easy to determine. Therefore, one needs a method which eliminates the influence of the inhomogeneity of the magnetic field. In the experiment we'll use two different methods which will be explained in the following.

Spin-echo-method The principle of the spin-echo-method is shown in figure (5). First, one applies a 90°-pulse so that the spins precess in the xy-plane around the z-axis. One sees that the transversal amplitude decays exponentially like we have discussed above. If we apply a 180°-pulse after time τ, the spins precess into other direction. Thus, the effect of the inhomogeneity of the magnetic field to the spins is inverted and one can see a second maximum after time τ. Finally, the ratio between the amplitudes of the two maximums yields the spin-spin relaxation time T_2.

CPMG-method The principle of the CPMG-method (Call-Purcell-Meiboom-Gill-method) is basically the same (see figure (5)). One eliminates the influence of the inhomogeneous magnetic field by inverting it with a 180°-pulse. The difference to the spin-echo-method is that in CPMG-method, several more 180°-pulse in time distance of 2τ are applied. Therefore, there are some more maximums, ideally exact at the middle between two 180°-pulses, and one gets more ratios between the amplitude of different maximums which causes a more exact result.
In reality, one cannot create a ideal 180°-pulse. This problem can be avoided by using different phase shifts between the 180°-pulses.

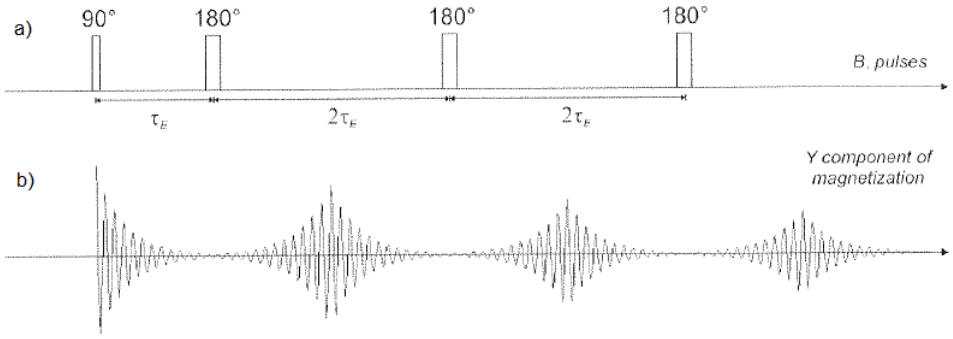

Figure 5: The sketch shows a) the pulse sequence and b) the resulting amplitudes. Note that in case of spin-echo-method only one 180°-pulse is applied and therefore, only one echo is measured. [Hal06]

3 The Experiment

3.1 The Set-Up

The experiment is set up by a polarisation coil, a B_1-coil and a gradient coil. The polarization coil is used to magnetize the analysed material perpendicular to the Earth's magnetic field. The B_1-coil generates the 90° and 180° pulses in order to flip the nuclear spins by the respective angular. The gradient coil itself consists of four smaller coils and generates a gradient field in x-, y- and z- direction.
The Coils are assembled into one another. The innermost coil is the B_1-coil, then the gradient coil and at the outermost the polarizing coil. The analysed liquids are put into a bottle that will be assembled in the B_1-coil.

3.2 The Execution

Since we measure the effects of the earth's magnetic field, which is approximately $46{\cdot}10^{-6}$T, on the spin-polarization it is extremely important to find a place that has a very low noise level. Therefore we set up the experiment in the coffee corner, where we have the least density of electro-magnetic fields caused by other experiments and the least amount metal causing inhomogeneities in the earth's magnetic field. Correspondingly we first monitored the noise:

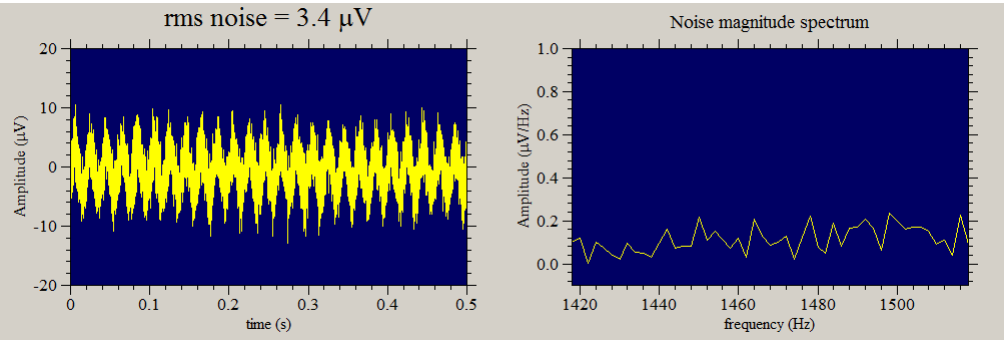

Figure 6: The image shows noise over time and noise over frequency

The Noise-level of $3.4\mu V$ is low enough to execute the experiment with sufficient accuracy.

3.3 Setting The Capacitance

The Analysing coil is connected with a variable capacitance, which leads to a amplitude gain dependent on the frequency. The resonance-frequency of a LC-circuit is
$\omega_0 = \frac{1}{\sqrt{LC}}$ Since the analysed spins rotate with a material-dependent frequency named LARMORfrequency we measured the coils resonance frequency on the capacitance:

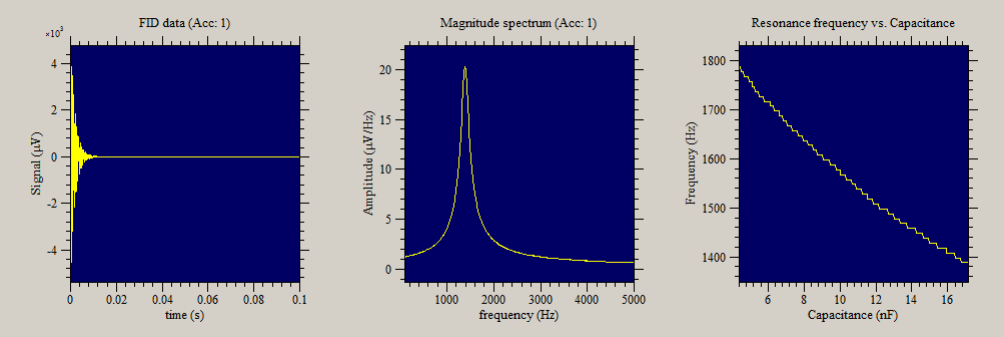

Figure 7: The image shows the capacitance-dependency of the coil

The first plot shows the oscillation of the voltage in the coil after a pulse. The amplitude decays due to the resistance of the electric components, which is called "ring-down" of the coil. The second plot shows the fourier-transformed of the oscillation, which lets us read out the resonance frequency gained by the current settings. The last plot displays the resonance frequency over capacitance.

To adjust the capacitance we analysed the spectrum using the "Pulse and Collect" routine of the program "Prospa". In the first measure showed two different peaks referring to the coils resonance frequency and the LARMOR-frequency of the probe. After that we changed the capacitance until the coils resonance frequency matched the LARMOR-frequency, which leads to a single peak in the plot:

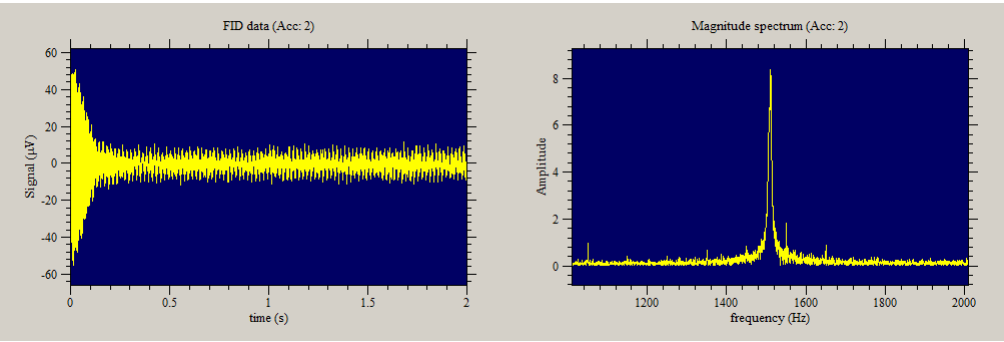

Figure 8: The image shows the resonance over frequency

We found a LARMOR-frequency of 1510Hz and a capacitance of 11nF for which the coils resonance frequency is 1510 Hz

3.4 Shimming

Since the earth's magnetic field is not completely homogeneous, we let the auto-shim routine of Prospa find the best parameters for the gradient coil. This leads to a higher amplitude of the resonance-peak. The aim was to get an amplitude higher than 30:

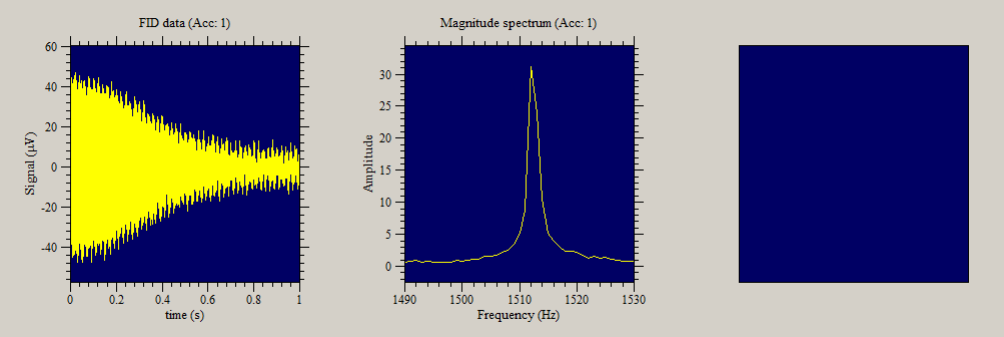

Figure 9: The image shows Plots made by the auto-shim routine

3.5 Finding The 90° And The 180° Pulse Duration

Prospa's "B1 Duration" routine measures the magnetisation of the analysed material after emitting pulses of various durations. By reading out the maximum and minimum of the amplitude over B1 plot we get the 90° and 180° pulse durations

$$t_{90} = 1.135ms \tag{14}$$

$$t_{180} = 2.1ms \tag{15}$$

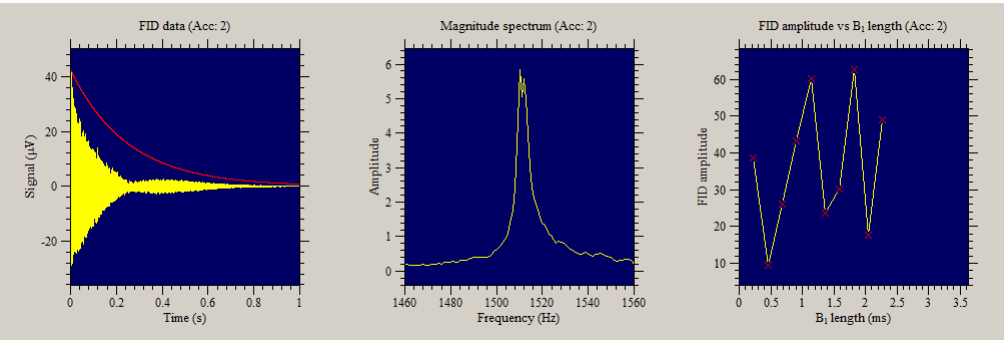

Figure 10: The image shows the Plots analysed to find out the 90° and 180° pulse durations

3.6 Measuring $T_{1,BE}$

At first we measured the T1 time $T_{1,BE}$, it takes the spins to relax after polarizing it parallel to the earth's magnetic field. Since the earth's magnetic field is much smaller then the polarizing field, the magnetization will decay to the net magnetization in earth's magnetic field alone. Since we can only measure the magnetization perpendicular to the z-axis, Prospa applies a 90° pulse after various times τ_i and afterwards measures the magnetization in the x-y-plane, which is proportional to the parallel magnetization before the pulse. With increasing τ_i, the aligned spins relax more and more and we measure an exponential decay.

The measured data was saved and fitted by a function $f(t) = a \cdot e^{-\frac{t}{T1}} + c$ to get the relaxation time T_1. Prospa displayed plots like the following:

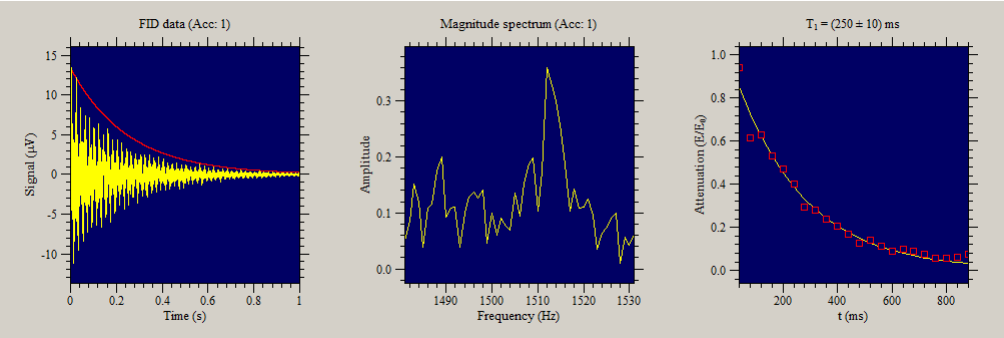

Figure 11: The image shows the Plots made by Prospa belonging to the $T_{1,BE}$ measurement of $CuSO_4$ (2000 $\frac{mol}{l}$)

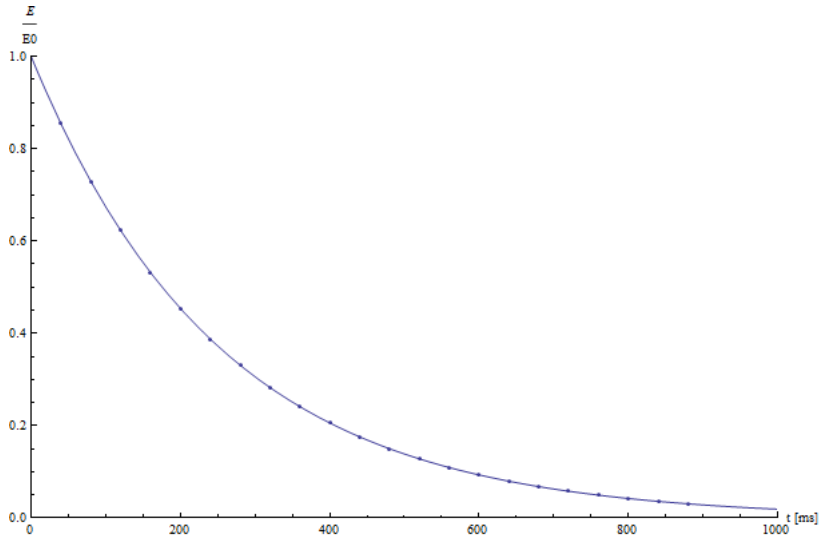

Figure 12: The image shows our fit of the Data belonging to the $T_{1,BE}$ measurement of $CuSO_4$ (2000 $\frac{\mu\,\mathrm{mol}}{\mathrm{l}}$)

The gained data is displayed in the following Table, where the $CuSO_4$ is only listed by its concentration in $\frac{\mu\,\mathrm{mol}}{\mathrm{l}}$

Table 1: Table With The Measured Relaxation Times $T_{1,BP}$

	Prospa	Own Fit
Substance	$T_{1,BE} \pm \delta T_{1,BE}$ [ms]	$T_{1,BE} \pm \delta T1_{1,BE}$ [ms]
Water	2500 ± 50	$2502,13 \pm 0,002$
Oil	126 ± 9	$126,4 \pm 0$
5000	120 ± 10	$85,66 \pm 4$
2000	250 ± 10	$253,24 \pm 0$
700	[5]	$607,57 \pm 0$
250	1110 ± 50	$1058,65 \pm 125$

[5]

3.7 Measuring $T1_{BP}$

To measure the Time $T_{1,BP}$ we polarize the Spins with a polarizing pulse of duration τ_p and apply a 90° pulse after the spins are aligned parallel to the earth's magnetic field again. This way we measure a Voltage V proportional to

$$V \propto V_0[1 - e^{-\frac{\tau_p}{T1}}]$$

The results were again fitted and analysed:

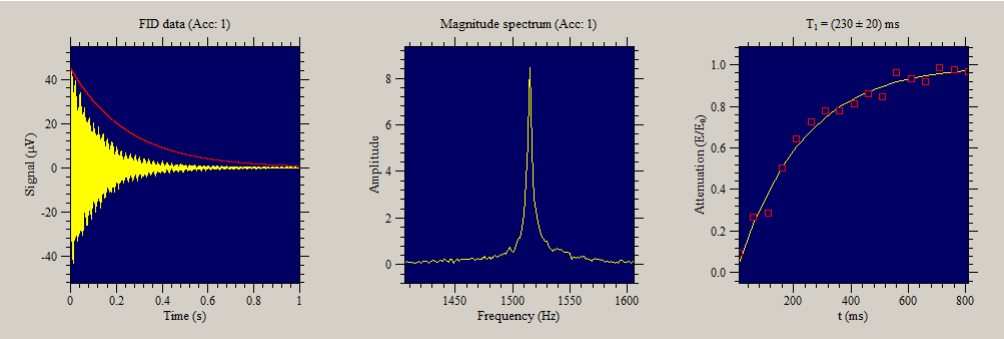

Figure 13: The image shows the Plots made by Prospa belonging to the $T_{1,BP}$ measurement of $CuSO_4$ (2000 $\frac{mol}{l}$)

[5] The data to the measure with $CuSO_4$ unfortunately got lost during the experiment

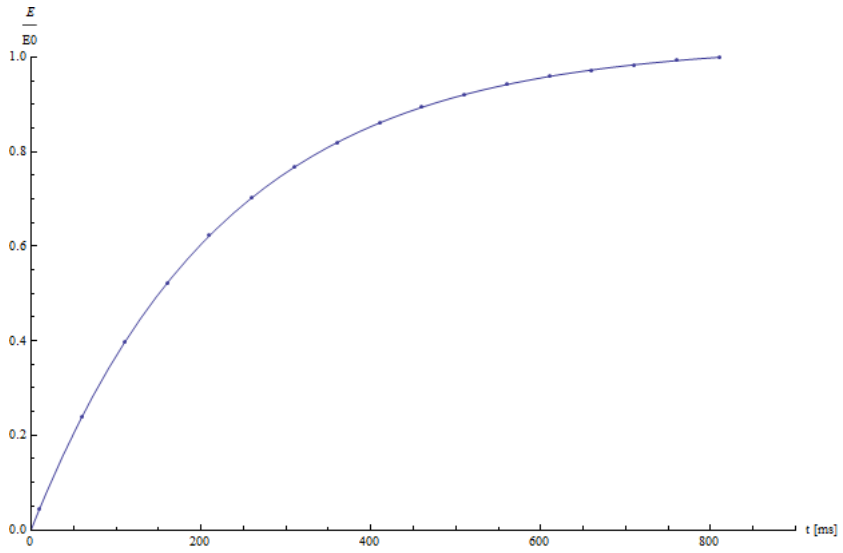

Figure 14: The image shows our fit of the Data belonging to the $T_{1,BP}$ measurement of $CuSO_4$ (2000 $\frac{\mu\,\mathrm{mol}}{\mathrm{l}}$)

Table 2: Table With The Measured Relaxation Times $T_{1,BP}$

	Prospa	Own Fit
Substance	$T_{1,BP} \pm \delta T_{1,BP}$ [ms]	$T1_{BP} \pm \delta T1_{BP}$ [ms]
Water	1000 ± 200	$1078,14 \pm 372$
Oil	86 ± 6	$103,29 \pm 10$
5000	90 ± 2	$89,9 \pm 0$
2000	220 ± 2	226 ± 0
700	380 ± 60	$377,6 \pm 0$
250	780 ± 80	1105 ± 220

3.8 Measuring T2

The time-constant $T2$ is characterised by the loss of phase coherence caused by spin-spin relaxation as a result of the magnetic moments of several spins interacting with each other. This is done by a Spin-echo measurement, where the Spins are polarized and flipped over into the x-y plane. The spins then start to dephase.
Attention should be paid to the fact that the spin relaxation time does alter if the surrounding magnetic field is inhomogeneous.

$$\frac{1}{T_2^*} = \frac{1}{T_2} + \gamma \Delta B \tag{16}$$

This effect however can be reversed by applying a 180° pulse after a Time τ_e, so that the spins flip over completely. This way the spins re-phase and measure a so called spin-echo.

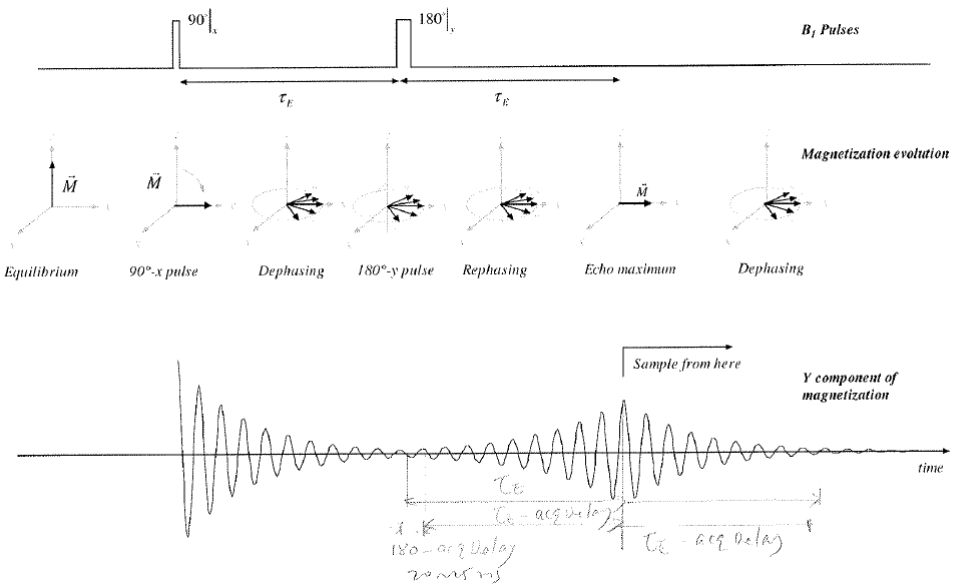

Figure 15: Diagram To Explain The Spin-Echo [Hal06]

Nevertheless, this method still has a downside. To get an accurate value for T_2, we need to know the exact 180° pulse duration. Prospa provides the CPMG-method to measure T_2. This method measures T_2 with varying 180° pulse durations in every single measure.

3.8.1 T_2 Spin Echo

The measured values were fitted with a function in the form of an exponential decay and got the following values [6]:

Table 3: Table With The Measured Relaxation Times T_2 With Spin-Echo Method

	Prospa	Own Fit
	$T2_{CPMG} \pm \delta T2_{CPMG}$ [ms]	$T2_{CMPG} \pm \delta T2_{CPMG}$ [ms]
Water	420 ± 40	2036 ± 0
5000	110 ± 20	118 ± 108
2000	250 ± 10	243 ± 73
700	480 ± 20	595 ± 83
250	750 ± 90	1915 ± 0

3.8.2 CPMG

The data gained in this experiment were analysed the same way as before [7]:

[6] Note, that this measurement was not done with oil
[7] Note, that this measurement was not done with oil

Table 4: Table With The Measured Relaxation Times T_2 With CPMG

	Prospa	Own Fit
	$T2 \pm \delta T2$ [ms]	$T2 \pm \delta T2$ [ms]
Water	2500 ± 50	423 ± 0
5000	180 ± 70	87 ± 11
2000	280 ± 4	216 ± 0
700	600 ± 100	471 ± 36
250	960 ± 100	625 ± 146

4 Analysis

4.1 Analysing T_1

At first we want to discuss the T_1 relaxation times. In Table 1 and 2 we can see, that water has the highest relaxation-time, meaning, that the spins in water take much longer to relax than the ones in oil. This means, that the spin-lattice-interaction of water is much lower, which is due to its low viscosity. This way the water molecules can maintain their energy much longer. This explains, why the relaxation time of the $CuSO_4$-solution decreases with higher concentration of $CuSO_4$. Another indication for that is, that the $CuSO_4$ solution with the low concentration of 250 $\frac{\mu mol}{l}$ has nearly the same relaxation time as water.

4.2 Analysing The Behaviour Of $CuSO_4$

Finally we want to analyse, how the measured relaxation times of the $CuSO_4$ depends on its concentration. Therefore we fit the measured data in a double logarithmic plot:

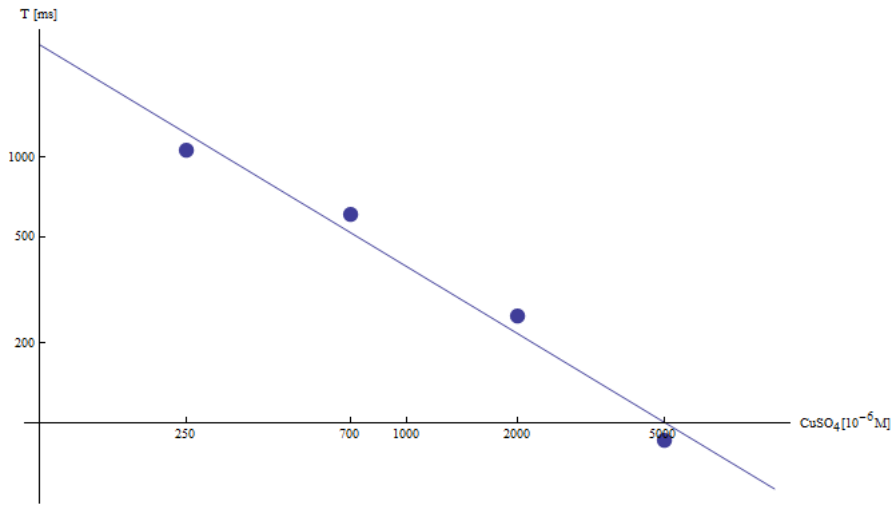

Figure 16: This double logarithmic plot shows the dependence of the relaxation time on the concentration of $CuSO_4$

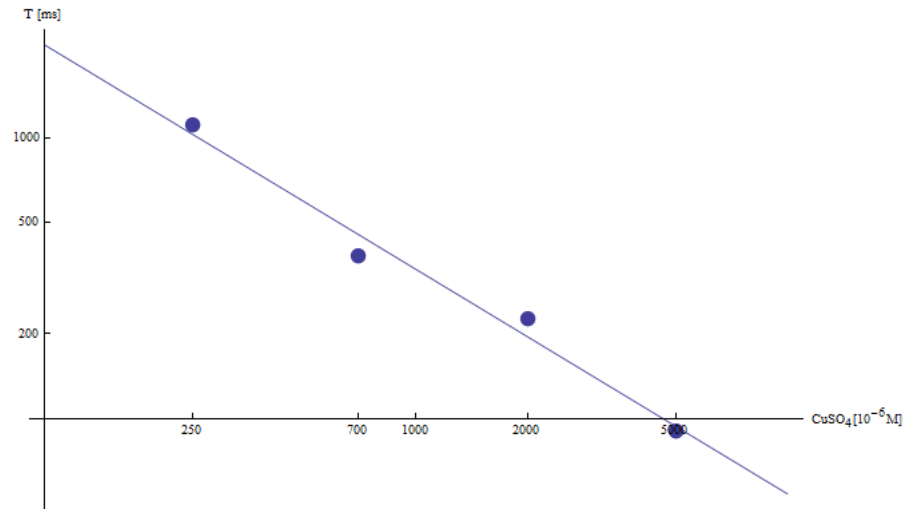

Figure 17: This double logarithmic plot shows the dependence of the relaxation time on the concentration of $CuSO_4$

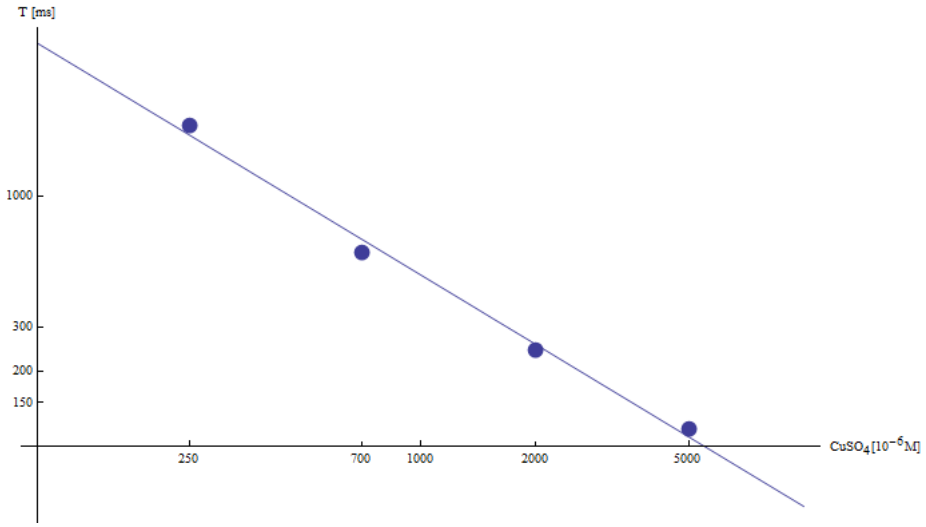

Figure 18: This double logarithmic plot shows the dependence of the relaxation time on the concentration of $CuSO_4$

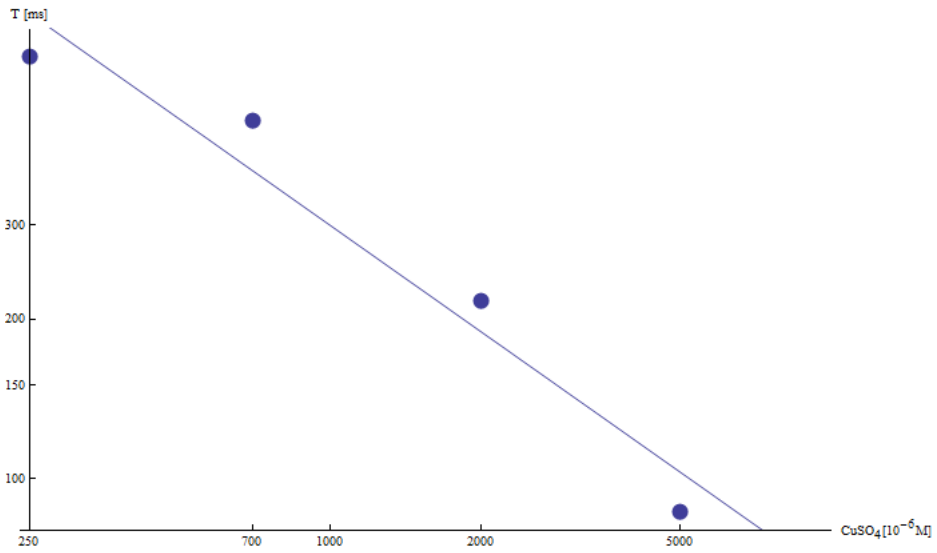

Figure 19: This double logarithmic plot shows the dependence of the relaxation time on the concentration of $CuSO_4$

The fits show a very good linear relation between the logarithms of the concentration and the spin-relaxation time of $CuSO_4$. This behaviour of $CuSO_4$ is the reason for its medicinal use as a contrast medium when it comes to Nuclear Magnetic Resonance. The very short relaxation time of $CuSO_4$ is a result of its strong ionic character, when solved in water. Due to the, compared to hydrogen bridge binding, very strong coulomb-interaction the ions are way better connected to the lattice, causing their magnetic moments to decay much faster.

4.3 Errors And Conclusion

Even though our results look quite good, there may have been some sources of error. Since some parts of the experiment were dependent on the earth's magnetic field, even the slightest interfering magnetic fields, as they are caused by mobile phones, could influence our measures. During the experiment for example, the dishwasher next to our set-up was running, and we had a laptop running constantly to do our measures.
Another source of errors are inhomogeneities in the earth's magnetic field caused by metallic objects in the surroundings. Especially the elevators cause huge inhomogeneities resulting in incorrect data, since they constantly chance their position, which makes it impossible to correct this by shimming.

Beside that, the main source of errors are probably the 90° and 180° pulse durations, that do not exactly match the literature values. Our measure hat various maxima and minima, nearly at the same height, which is why we could not measure those durations very well. And since most of our measures depend on those pulse durations, they are probably the main source of error.
Nevertheless we got very clear measurements, meaning, that our data show the exponential

coherences very good and the results clearly show the dependence of the relaxation times on the concentration of $CuSO_4$.
All in all the experiment shows the qualitative relations between the nature of the analysed substances and the behaviour of their spins. It also gives a good insight in the way, spins interact with each other and with their environment.

showed good results, even though the measured 90° and 180° pulse durations did not match the literature values. The wrong values could be

5 Attachment - Fits

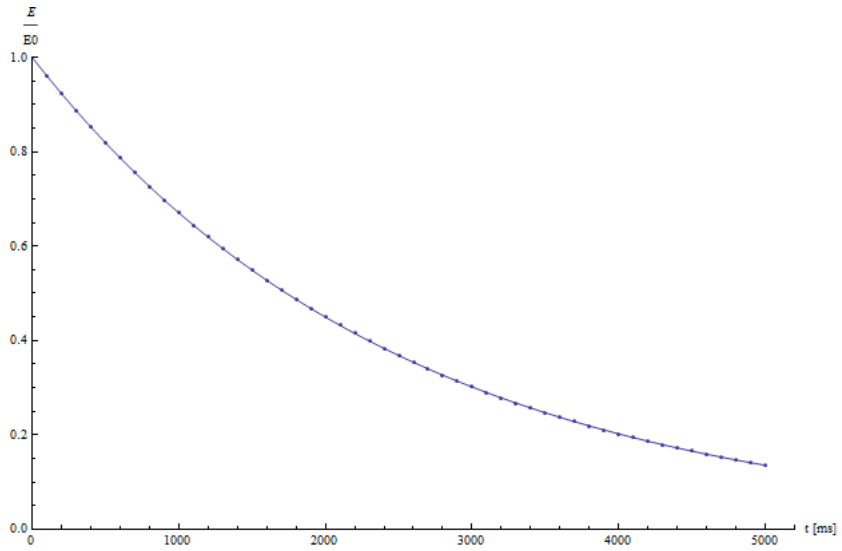

Figure 20: $T_{1,BE}$ fit for water

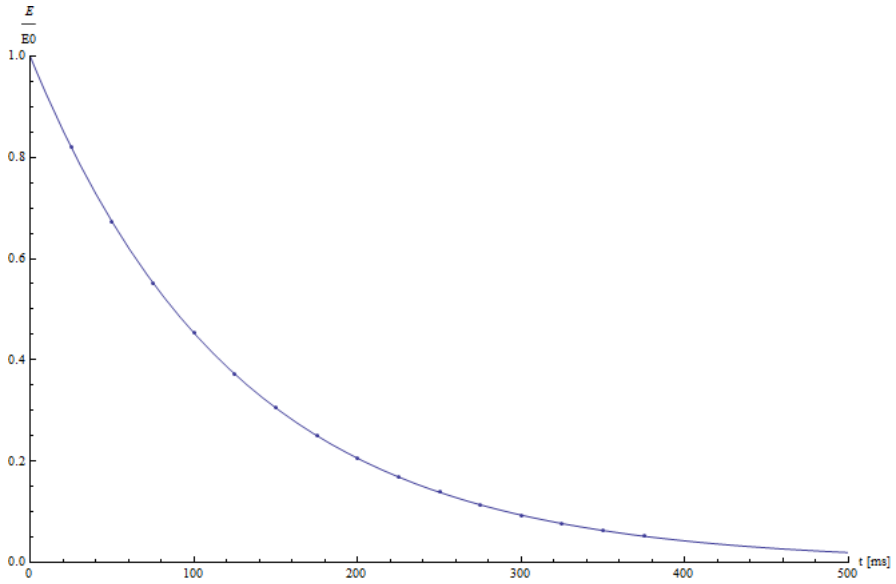

Figure 21: $T_{1,BE}$ fit for oil

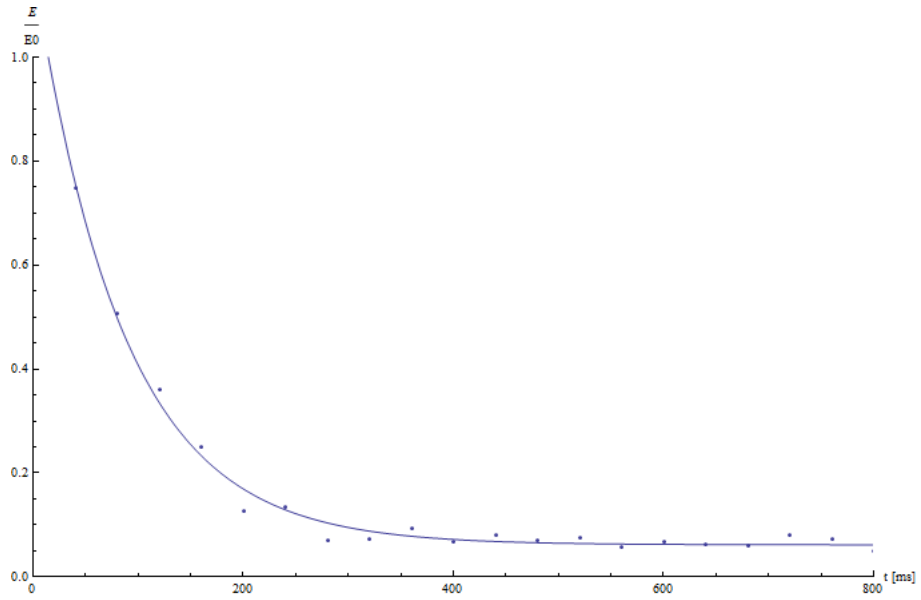

Figure 22: $T_{1,BE}$ fit for $CuSO_4$ 5000$\frac{\mu\,\mathrm{mol}}{l}$

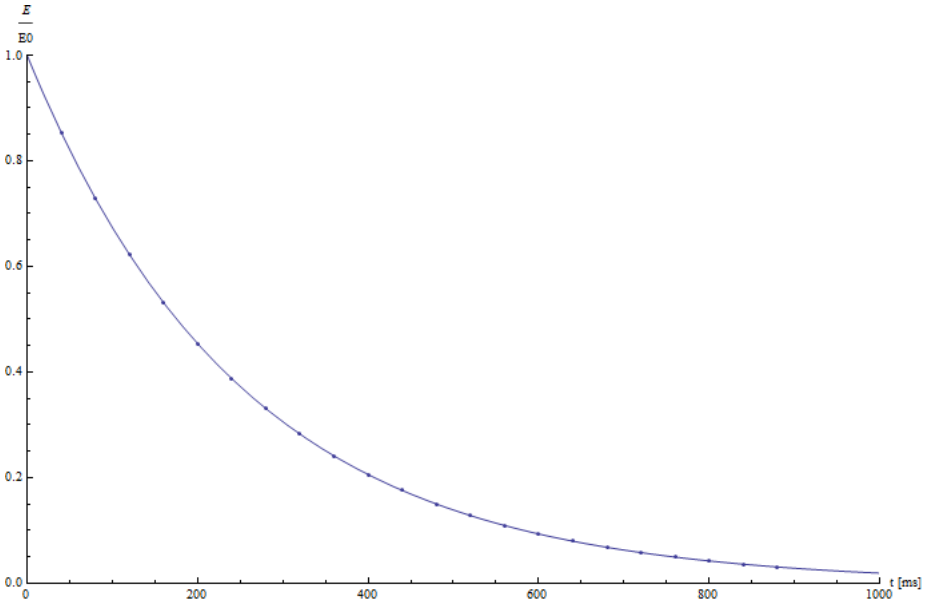

Figure 23: $T_{1,BE}$ fit for $CuSO_4$ 2000$\frac{\mu\,\mathrm{mol}}{l}$

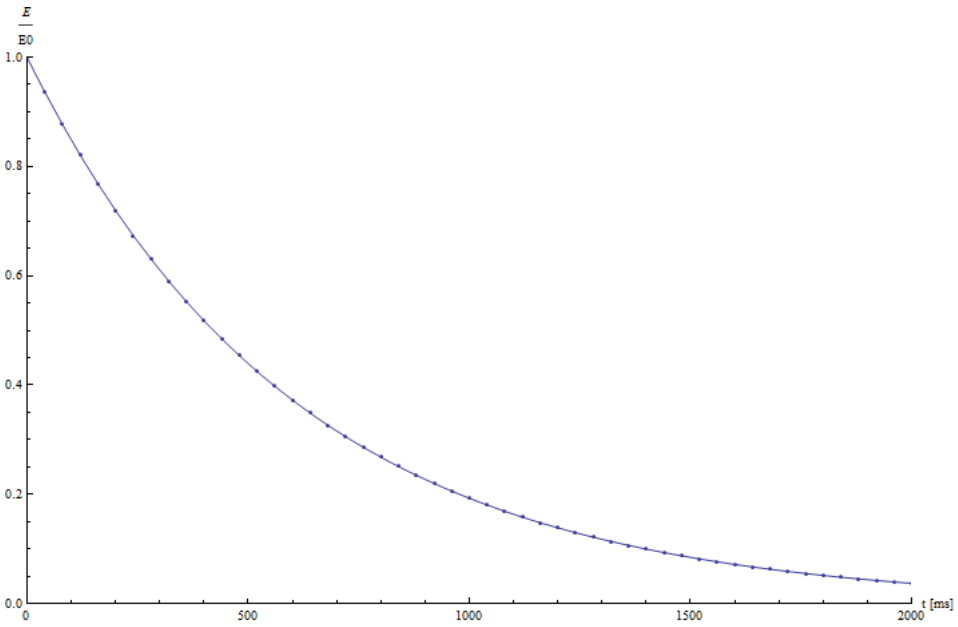

Figure 24: $T_{1,BE}$ fit for $CuSO_4$ $700\frac{\mu\,\mathrm{mol}}{l}$

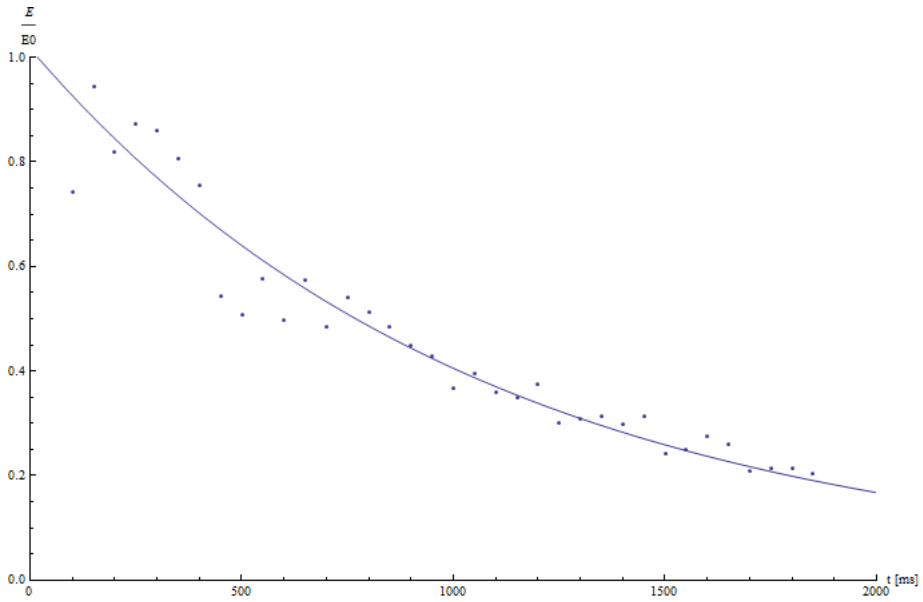

Figure 25: $T_{1,BE}$ fit for $CuSO_4$ $250\frac{\mu\,\mathrm{mol}}{l}$

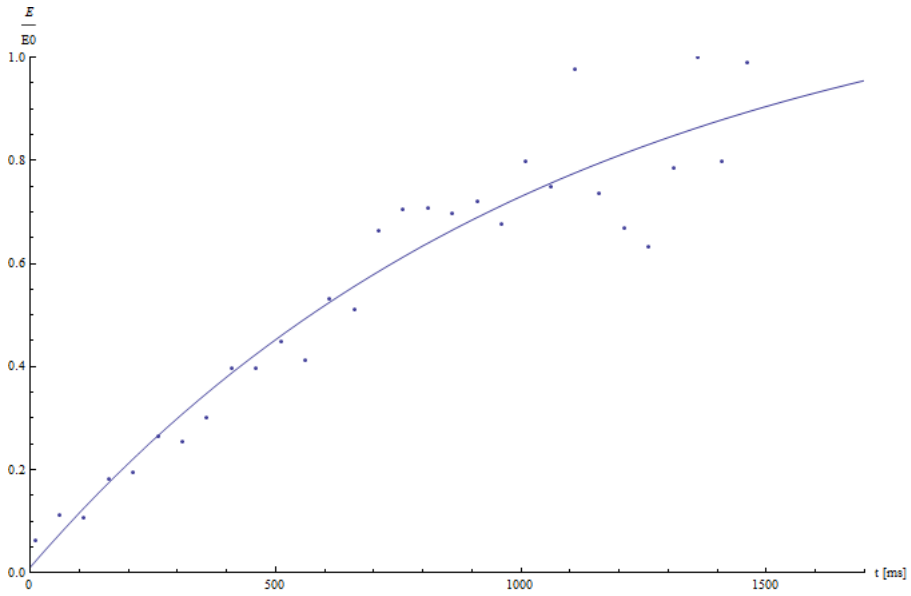

Figure 26: $T_{1,BP}$ fit for water

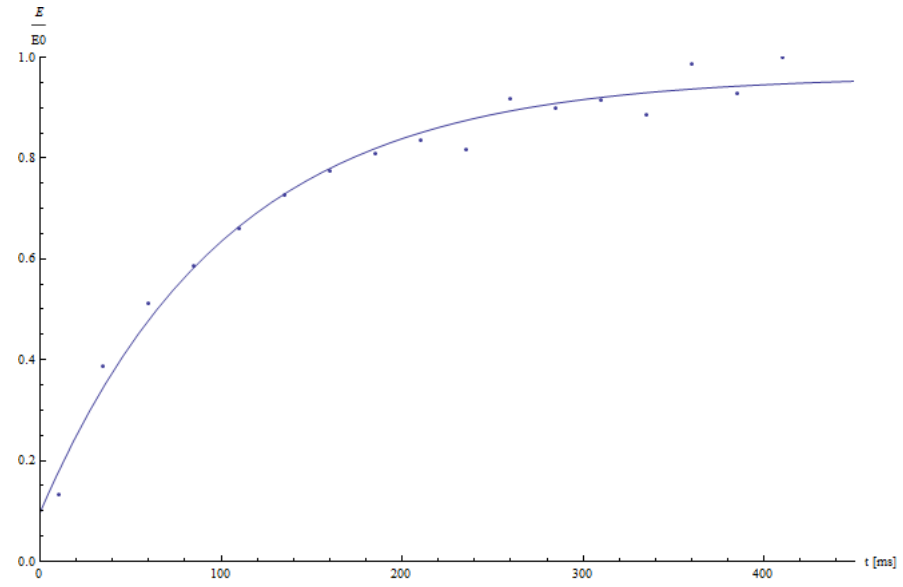

Figure 27: $T_{1,BP}$ fit for oil

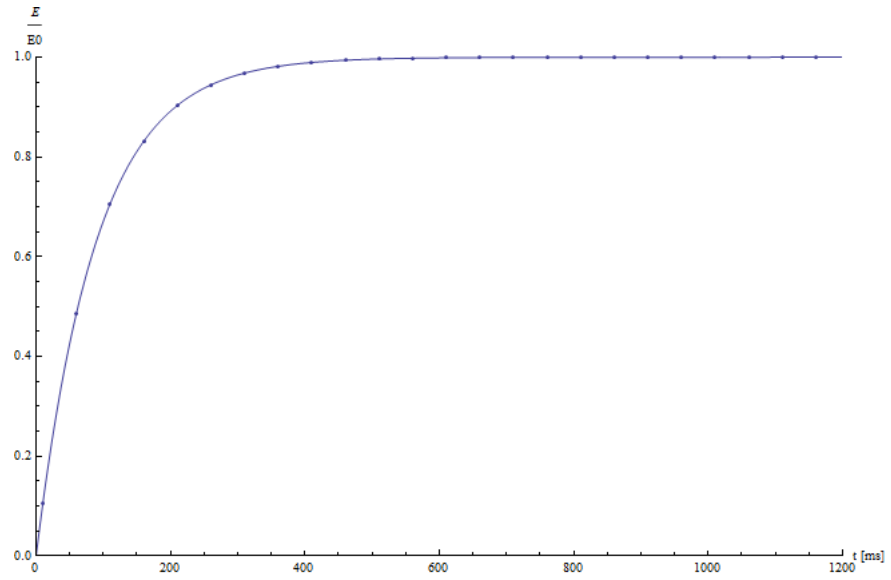

Figure 28: $T_{1,BP}$ fit for $CuSO_4$ $5000\frac{\mu\,\mathrm{mol}}{l}$

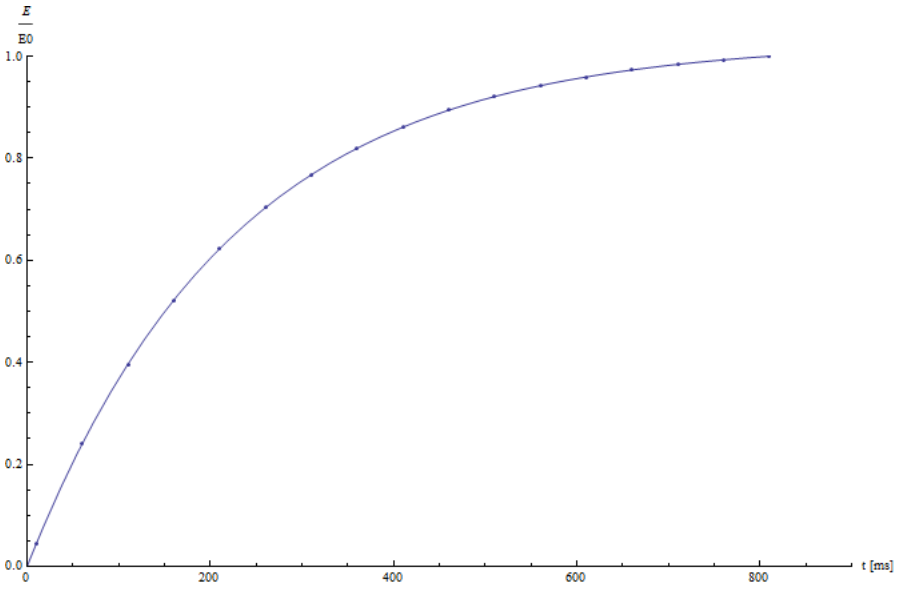

Figure 29: $T_{1,BP}$ fit for $CuSO_4$ $2000\frac{\mu\,\mathrm{mol}}{l}$

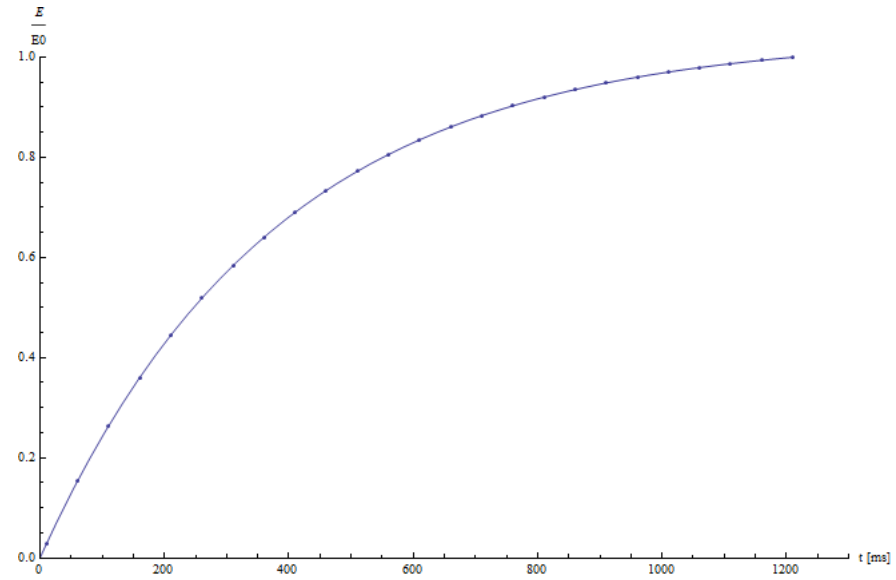

Figure 30: $T_{1,BP}$ fit for $CuSO_4$ $700\frac{\mu\,\mathrm{mol}}{l}$

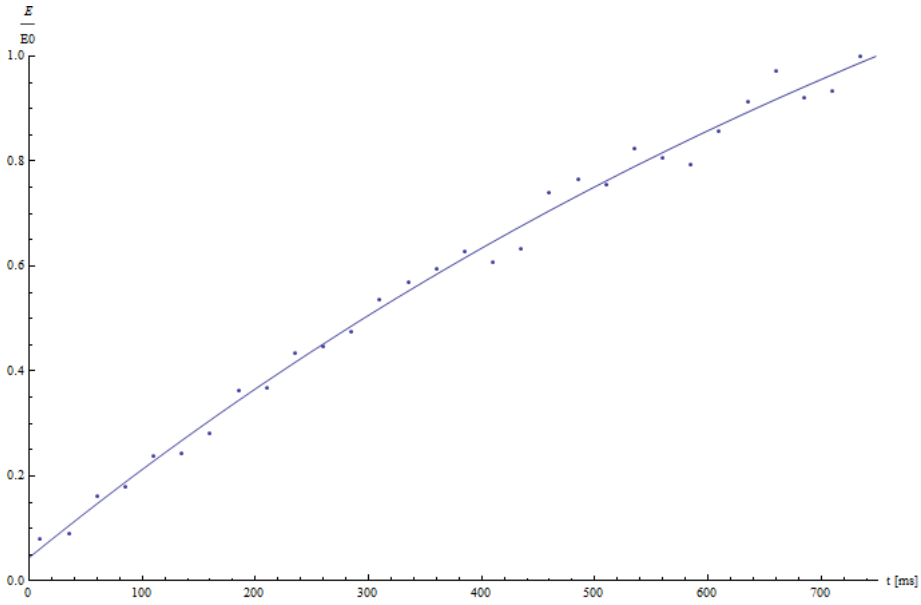

Figure 31: $T_{1,BP}$ fit for $CuSO_4$ $250\frac{\mu\,\mathrm{mol}}{l}$

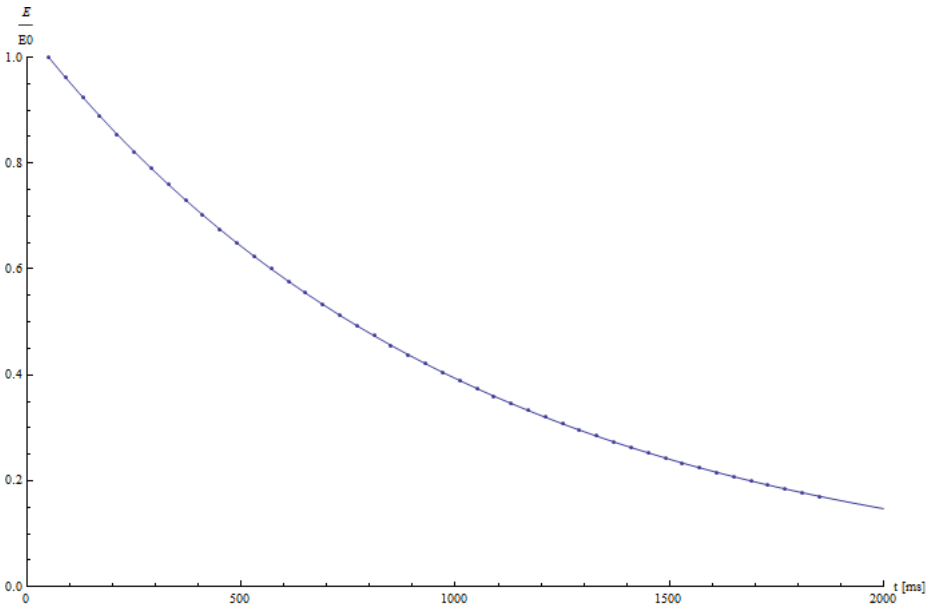

Figure 32: T_2 spin-echo method fit for water

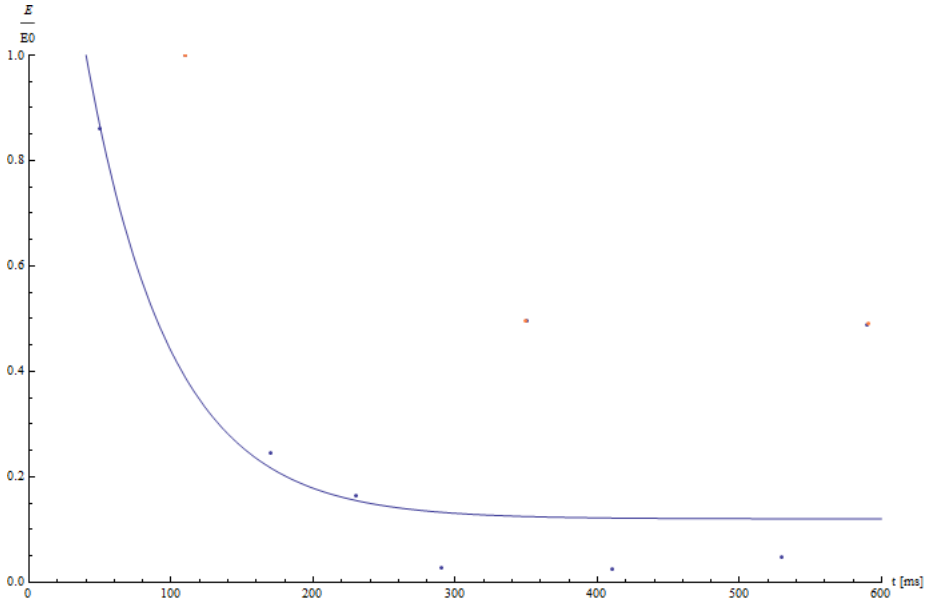

Figure 33: T_2 spin-echo method fit for $CuSO_4$ $5000\frac{\mu\,\mathrm{mol}}{l}$

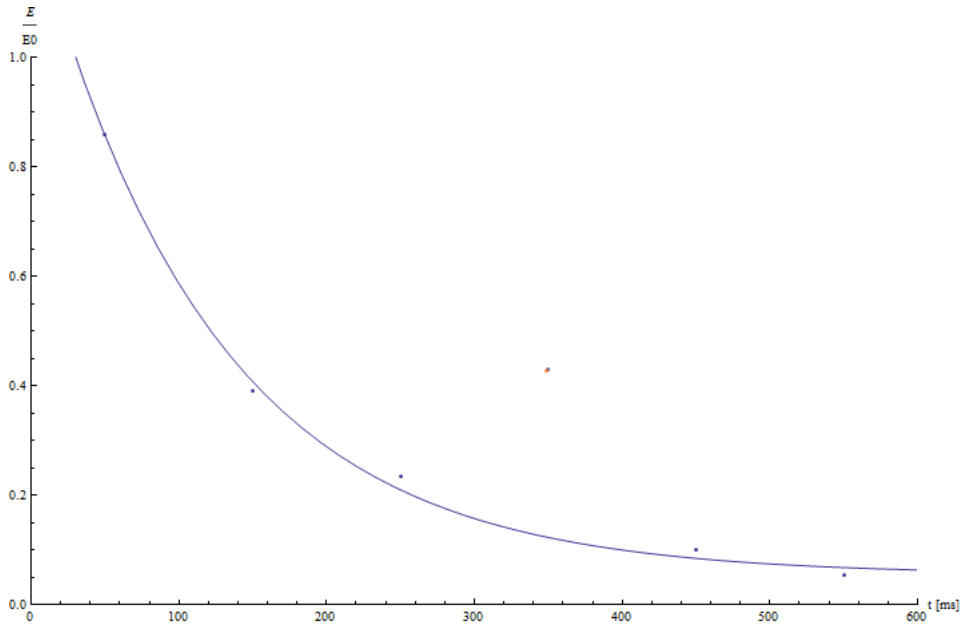

Figure 34: T_2 spin-echo method fit for $CuSO_4$ $2000\frac{\mu\,\mathrm{mol}}{l}$

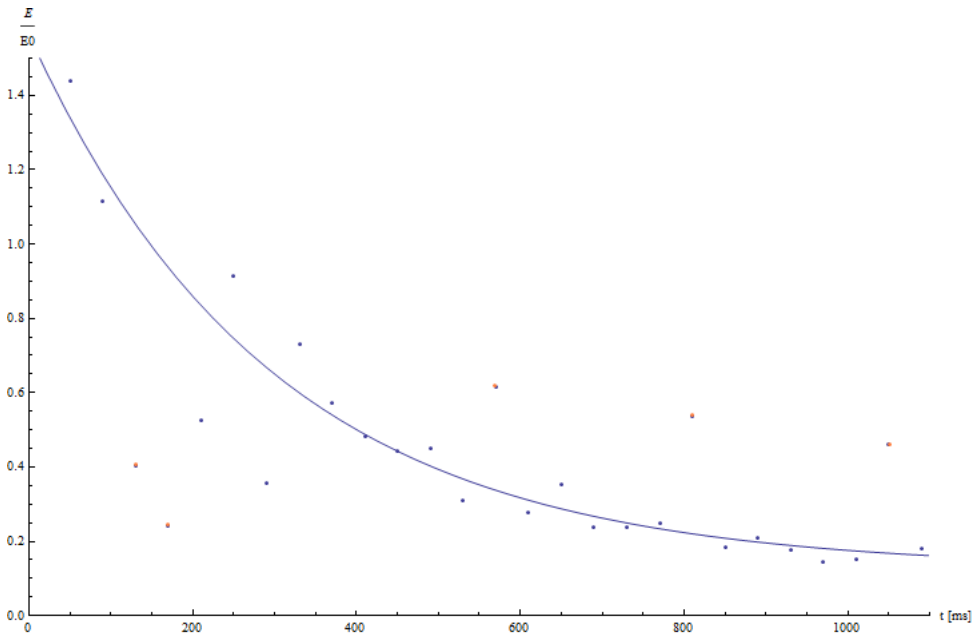

Figure 35: T_2 spin-echo method fit for $CuSO_4$ $700\frac{\mu\,\mathrm{mol}}{l}$

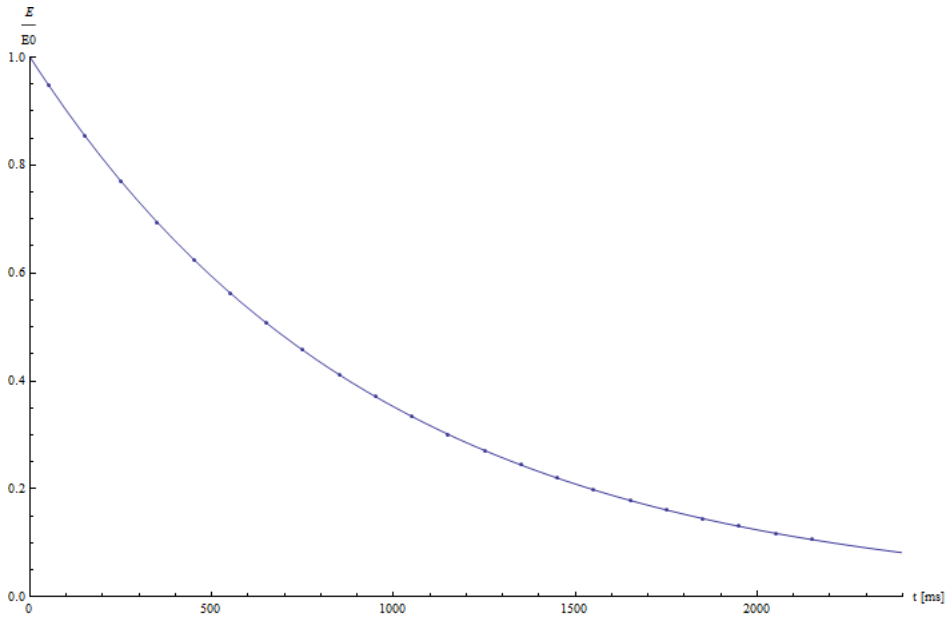

Figure 36: T_2 spin-echo method fit for $CuSO_4$ $250\frac{\mu\,\mathrm{mol}}{l}$

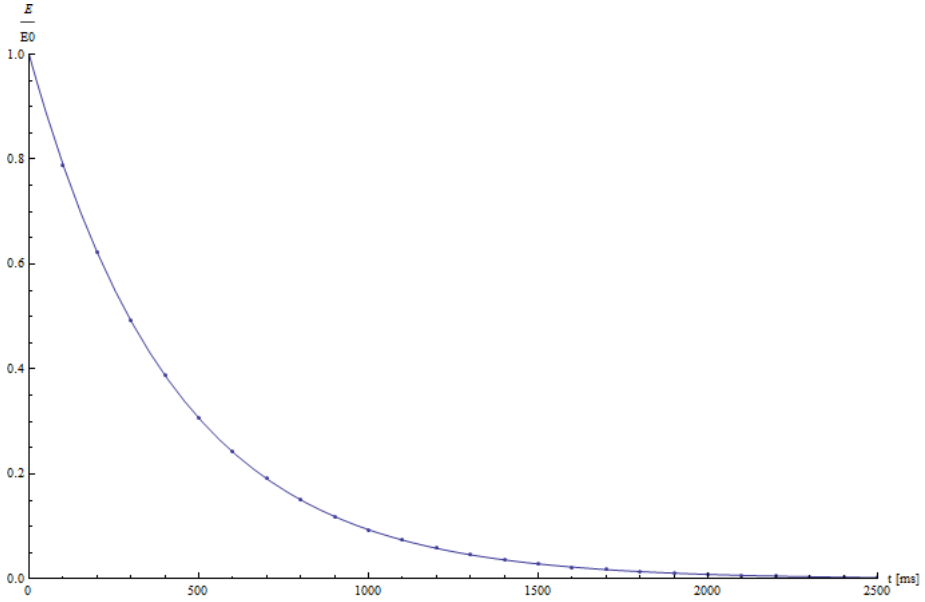

Figure 37: T_2 CPMG method fit for water

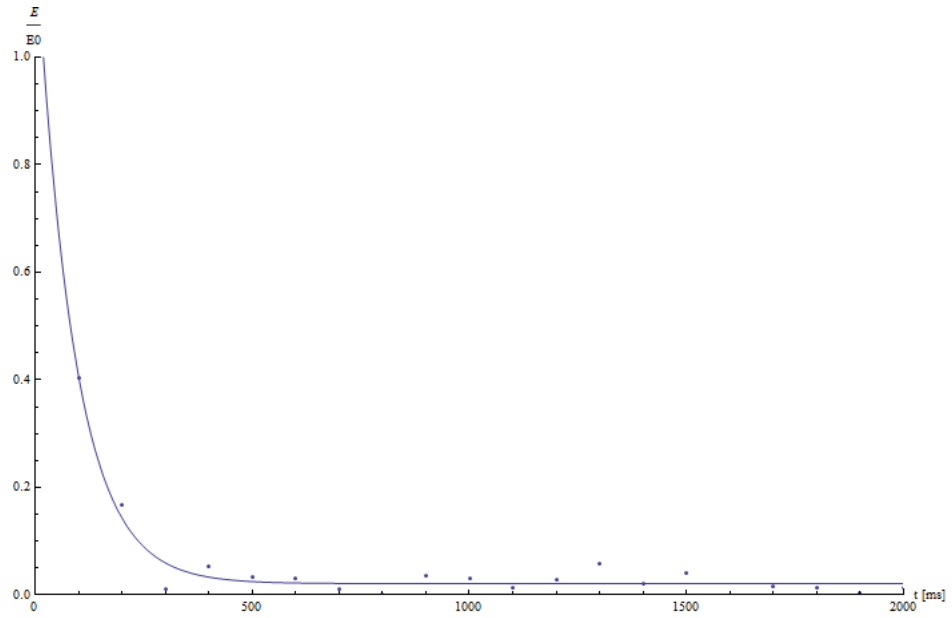

Figure 38: T_2 CPMG method fit for $CuSO_4$ $5000\frac{\mu\,\mathrm{mol}}{l}$

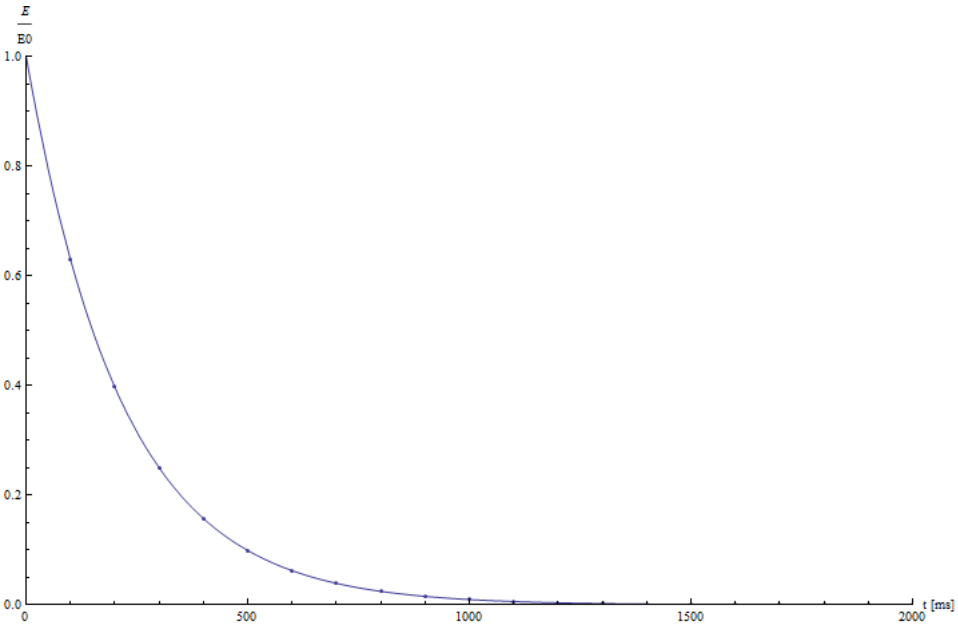

Figure 39: T_2 CPMG method fit for $CuSO_4$ $2000\frac{\mu\,\mathrm{mol}}{l}$

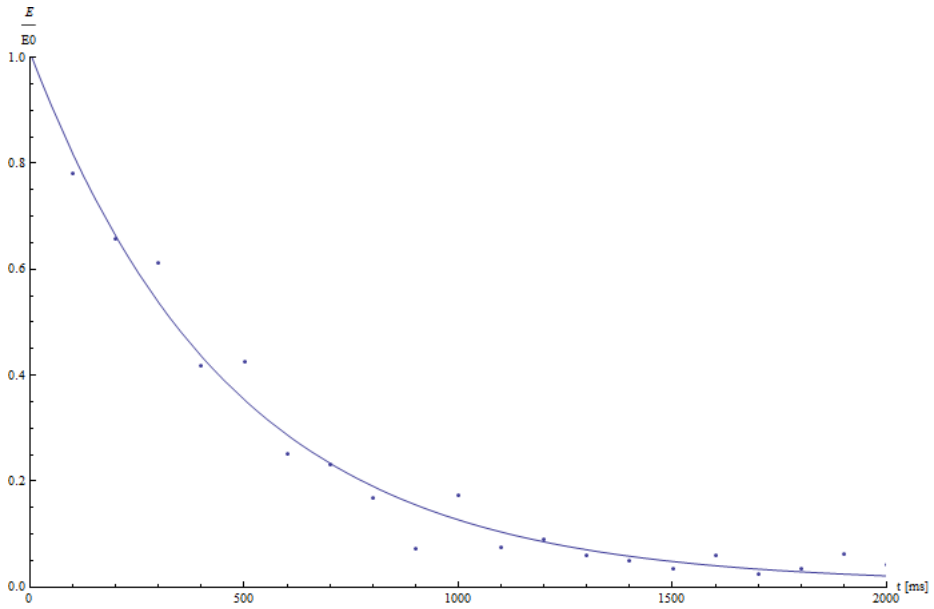

Figure 40: T_2 CPMG method fit for $CuSO_4$ $700\frac{\mu\,\mathrm{mol}}{l}$

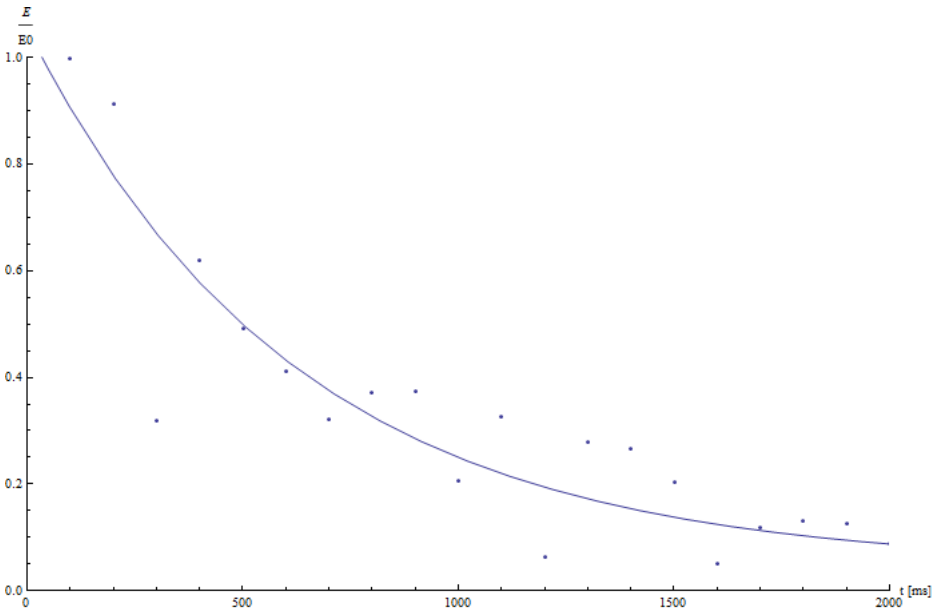

Figure 41: T_2 CPMG method fit for $CuSO_4$ $250\frac{\mu\,\mathrm{mol}}{l}$

References

[Bau13] Bausinger, Ralf: *Nuclear magnetic resonance in the Earth's magnetic field - manual*, 2013

[Hal06] Halse, Meghan A.: *Terranova-MRI EFNMR Student Guide*, Limited Edition, 2006

[Dem10] Demtröder, Wolfgang: *Experimentalphysik 3: Atome, Moleküle und Festkörper*, 4th edition, Springer-Verlag, 2010

[Har83] Harris, Robin K.: *Nuclear Magnetic Resonance Spectroscopy: A Physiochemical View*, Pitman Books, 1983

[Mic81] Michel, Dieter: *Grundlagen der kernmagnetischen Resonanz*, Akademie-Verl., 1981

[TUD09] Scheuermann; Gädke; Lusceac; Geil; Fujara: *Magnetische Kernspinresonanz zum Studium der molekularen Dynamik*, 2009

[Wik13] Wikipedia - free encyclopaedia, articles: Kernspinresonanz, Relaxation, Bloch-Gleichungen , 25.01.2012

[UM13] http://qgp.uni-muenster.de/ jowessel/pages/teaching/ss03/seminar/andela.pdf , 25.01.2012

[UT13] http://www.pit.physik.uni-tuebingen.de/PIT-II/teaching/ExPhys-V_WS03-04/ExP-V%283%29-Kap5_5-Magnetismus-Magnetische%20Resonanz.pdf , 25.01.2012

[UD13] http://www.nmr.uni-duesseldorf.de/pics/th_fig3.gif , 25.01.2013

List of Figures

List of Tables